Published in final edited form as:
J Proteomics. 2012 December 21; 77: 87–100. doi:10.1016/j.jprot.2012.07.009.

An optimized isolation of biotinylated cell surface proteins reveals novel players in cancer metastasis

Piia-Riitta Karhemo[a,h], **Suvi Ravela**[b], **Marko Laakso**[c], **Ilja Ritamo**[d], **Olga Tatti**[a,e,h], **Selina Mäkinen**[a,h], **Steve Goodison**[f], **Ulf-Håkan Stenman**[b], **Erkki Hölttä**[e], **Sampsa Hautaniemi**[c], **Leena Valmu**[d], **Kaisa Lehti**[c,e], and **Pirjo Laakkonen**[a,g,h,*]

[a]Research Programs Unit, Molecular Cancer Biology, Biomedicum Helsinki, University of Helsinki, Finland [b]Department of Clinical Chemistry, University of Helsinki, Finland [c]Research Programs Unit, Genome Scale Biology, Biomedicum Helsinki, University of Helsinki, Finland [d]Finnish Red Cross Blood Services, Finland [e]Department of Pathology, Haartman Institute, University of Helsinki, Finland [f]MD. Anderson Cancer Center-Orlando, FL, USA [g]Foundation for the Finnish Cancer Institute, Finland [h]Institute of Biomedicine, University of Helsinki, Finland

Abstract

Details of metastasis, the deadliest aspect of cancer, are unclear. Cell surface proteins play central roles in adhesive contacts between the tumor cell and the stroma during metastasis. We optimized a fast, small-scale isolation of biotinylated cell surface proteins to reveal novel metastasis-associated players froman isogenic pair of human MDA-MB-435 cancer cells with opposite metastatic phenotypes. Isolated proteins were trypsin digested and analyzed using LC–MS/MS followed by quantitation with the Progenesis LC–MS software. Sixteen proteins displayed over twofold expression differences between the metastatic and non-metastatic cells. Interestingly, overexpression of most of them (14/16) in the metastatic cells indicates a gain of novel surface protein profile as compared to the non-metastatic one. All five validated, differentially expressed proteins showed higher expression in the metastatic cells in culture, and four of these were further validated in vivo. Moreover, we analyzed the expression of two of the identified proteins, CD109 and ITGA6 in 3-dimensional cultures of six melanoma cell lines. Both proteins marked the surface of cells derived from melanoma metastasis over cells derived from primary melanoma. These unbiased identification and validation of both known and novel metastasis-associated proteins indicate a reliable approach for the identification of differentially expressed surface proteins.

Keywords

Cell surface; Biotinylation; Metastasis; CD109; ITGA6; LC–MS/MS

1. Introduction

A hallmark of the malignant process is the acquisition of an invasive phenotype that allows neoplastic cells to invade the surrounding tissue and disseminate into specific organs. Metastatic spread of cancer is the most serious challenge for cancer treatment and the metastatic dissemination, rather than the primary tumor, is responsible for 90% of cancer

[*]*Corresponding author*. Tel.: +358 9 19125537; fax: +358 9 19125510. pirjo.laakkonen@helsinki.fi (P. Laakkonen).

Supplementary data to this article can be found online at http://dx.doi.org/10.1016/j.jprot.2012.07.009.

deaths. The details of the multistep process leading to metastatic disease are not fully understood. A cancer cell must detach from the primary tumor, invade the lymphatics and/or blood vessels to be transported to distant organs where it must adhere, extravasate, and proliferate to form a metastatic lesion [1]. In addition, tumor cells can stay dormant (no proliferation or apoptosis) at the distant site and metastases can occur decades after the primary treatment [2]. Organ specific colonization of tumors leads to metastasis in a different set of organs by different tumor types. For example breast cancers frequently metastasize to the lung and liver, and also to the bone marrow and brain while in the case of prostate cancer bone metastases are often the only site for distant lesions [3–5].

The cell surface proteins represent ideal targets for novel therapies due to their accessibility. Currently, two-thirds of the protein-based drug targets are located at the cell surface while cell surface proteins represent only about 22% of all proteins in the human genome [6, 7]. These proteins are underrepresented in proteomics analyses performed from whole cell extracts due to their low abundance and poor solubility. Cell fractionation and analysis of a subcellular proteome reduce the sample complexity allowing an in-depth analysis resulting in identification of more intermediate and low abundant proteins [8].

Several methods have been used to fractionate cell extracts and enrich the cell surface and/or plasma membrane proteins. All proteins at the cell surface are not classified as plasma membrane proteins and vice versa. For example ligands bound to their receptors can be classified as cell surface proteins but not as true plasma membrane proteins because they lack direct contact with it. The most commonly used methods for the isolation of plasma membrane proteins can be classified into a) homogenization combined to membrane density separation and b) affinity isolation of tagged membrane proteins [9, 10]. Plasma membrane proteins have also been isolated with the aid of electrostatic attachment of cationic colloidal silica to the membranes [11] combined with Triton X-114 phase partitioning [12]. Cell surface proteins can easily be tagged with a membrane-impermeable biotin [13]. This allows the usage of streptavidin-linked beads for the isolation of the biotin-labeled proteins from the cell extracts. As most secreted and cell surface proteins are glycosylated the cell surface capture technique (CSC), which covalently labels extracellular glycanmoieties on live cells, has also successfully been applied to isolate the cell surface glycoproteome [14]. However, these two methods (cell surface tagging with biotin and CSC) are not limited only to the isolation of plasma membrane proteins. Glycoproteins and proteins accessible for the labeling reagent e.g. extracellular matrix proteins of the adherent cells as well as the ligands bound to their receptors are isolated and analyzed with downstream applications.

Extracellular matrix, cell surface and secreted proteins play central roles in the signaling and adhesive interactions between the tumor and stromal cells during the various stages of metastasis and during the organ specific homing of metastatic cells [15–18]. Therefore, we compared the biotinylated cell surface fractions of metastatic and non-metastatic cells to identify proteins associated with the metastatic process. We used an isogenic pair of the human MDA-MB-435 cancer cell line as a model [19, 20] since the differential expression of a protein is more likely to be associated to the metastatic behavior than when using non-isogenic cell lines. Of these subclones one tumor cell line colonizes the lungs while the other remains as a single cell and fails to proliferate and form lung metastases [20]. The MDA-MB-435 cell line was originally considered as breast carcinoma, but microarray data suggests that it may be of melanoma origin [21–23]. Recent reports claim again that the cell line would be a breast carcinoma [24, 25]. However, the common origin of these cell lines enables the comparative investigation of cellular and molecular events in the metastatic process in a stable well-characterized model [26–28].

Previously, ultracentrifuged and density separated plasma membrane fractions of these cell lines have been analyzed [29]. A pure plasma membrane fraction devoid of other cellular compartments is, however, difficult to obtain by using the ultracentrifugation method [30]. In addition, plasma membrane proteins residing in the intracellular compartment will be isolated and analyzed. In this work we aimed to identify novel metastasis associated cell surface/extracellular proteins and molecular pathways for future functional studies. To this end we optimized a fast, small-scale isolation of the biotinylated cell surface proteins and performed a label free quantitative proteomics analysis by using the metastatic and non-metastatic subclones of the human MDA-MB-435 cancer cell line. Inherent to the procedure of protein isolation (biotinylation versus homogenization combined to membrane density separation), the metastasis-associated cell surface proteome obtained in our analysis differed from the previously reported one adding novel information to the field of metastasis.

2. Materials and methods

2.1. 2D- and 3D cell cultures

Melanoma cells (WM164, WM165, WM793, WM852, G361 and Bowes) were grown in MEM-medium supplemented with 10% FCS, 1% glutamine and penicillin–streptomycin. The MDA-MB-435 derived subclones were grown in RPMI-1640 medium supplemented with 10% FCS, 1% glutamine and penicillin–streptomycin. The collagen and fibrin 3D growth assays were performed as described [31].

2.2. Cell surface protein isolation

The isolation of cell surface proteins was modified from [32] and [33]. Cells were plated on a 10 cm cell culture dish 3 days prior to the cell surface protein isolation. We used one plate/isolation. Cells were washed three times with Dulbecco (PBS+0.901 mM $CaCl_2$+0.492 mM $MgCl_2$) followed by a 30-minute incubation with EZ-Link Sulfo-NHS-SS-Biotin (Pierce, Rockford, IL, USA; 0.5 mg/ml in Dulbecco) on ice. Cells were washed twice with Dulbecco and the non-reacted biotin was blocked with 20 mM glycine for 15 minutes. To prevent the reduction of the disulfide bridge in the biotin molecule during the cell lysis, a 100 μM oxidized glutathione (Sigma-Aldrich, St. Louis, MO) was added in the last wash solution. For cell lysis 500 μl of lysis buffer (2% NP-40, 1% Triton X-100, 10% glycerol, 100 μM oxidized glutathione, EDTA free protease inhibitor tablet (Roche, Mannheim, Germany)) in PBS was added to the cells. Lysed cell extracts were scraped off the plates and transferred to an Eppendorf tube followed by incubation on ice on a shaker for 30 min. The cell extracts were incubated with 30 U of DNase (22 °C 50 min, Roche, Mannheim, Germany) and centrifuged for 20 min (20800×*g*, at +4 °C) to pellet the insoluble material. The protein concentration of the supernatants was determined using the DC-(Bio-Rad, Hercules, CA, USA) or BCA-(Thermo Fisher Scientific, Pierce Rockford, IL, USA) protein assays. Equala mounts of protein (~2 mg) from each extract were used for cell surface protein isolation. The supernatant was pre-cleared using biotin agarose beads (ImmunoPure® Immobilized D-biotin, Pierce, Rockford, IL, USA) and pre-cleared solution was used for the cell surface protein isolation using magnetic streptavidin beads (Dynabeads®MyOne™ Streptavidin, Invitrogen Dynal, AS, Norway). Beads were washed four times with the lysis buffer, four times with 300 mM NaCl in lysis buffer and twice with 50 mM Tris–HCl, pH 7.8. Proteins were eluted twice with an elution buffer (50 mM DTT in 50 mM Tris–HCl, pH 7.8) at 30 °C, followed by pooling of the eluates. Three biological replicates and one non-biotinylated control from each cell line were used in the study.

2.3. LC–MS/MS-analysis

Proteins were digested with trypsin (sequence grade modified, Promega, Madison, WI, USA) and prepared for the mass spectrometry analysis as previously described [34].

Digested proteins were analyzed by LC–MS/MS. Peptides were loaded to a reversed phase pre-column (NanoEase Atlantis dC18, 180 μm × 23.5 mm, Waters, Milford, MA, USA) with 0.1% formic acid and separated in reversed phase analytical column (PepMap 100, 75 μm × 150 mm, Thermo Fisher Scientific Dionex, Germerin, Germany) with a linear gradient (4–50%) of 95% acetonitrile in 0.08% formic acid in 35 min. The Ultimate 3000 liquid chromatography instrument (Thermo Fisher Scientific Dionex, Germerin, Germany) was operated in nano scale with a flow rate of 0.3 μl/min. Both the pre-column and the analytical column were kept at 30 °C. Eluted peptides were introduced to an LTQ Orbitrap XL mass spectrometer (Thermo Fisher Scientific Inc.) via the ESI Chip interface (Advion BioSciences Inc.) in the positive-ion mode. The mass spectrometer was calibrated with a Thermo Fisher Scientific standard LTQ calibration solution consisting of caffeine, MRFA tetrapeptide and Ultramark 1621. The instrument was tuned with glu-fibrinopeptide B (Sigma-Aldrich, St. Louis, MO, USA). Full scan for eluting peptides was acquired in the mass range of 300–2000 m/z on the Orbitrap-detector with 60 000 resolution (FWHM) at 400 m/z, the AGC target was set to 200 000 and the maximum inject time to 800 ms. Based on full scan, six MS/MS data-dependent scans were acquired on LTQ with the AGC target set to 10 000 and the maximum inject time set to 100 ms. An isolation width of 2 m/z was used for precursor selection. Normalized collision energy of 35%, activation time of 100 ms and activation Q set to 0.25 were used for peptide fragmentation. Precursors, whose charge state couldn't be determined or charge state was +1, were discarded from the MS/MS analysis. Precursors were dynamically excluded for 10 s with a repeat count of 1. Both full scan and MS/MS scans consisted of one microscan and they were acquired as profile data.

2.4. Data analysis and quantitation in the Progenesis LC–MS software

For the differential expression analysis the mass spectrometer raw-files were transformed to .mzxml with ReAdw-program (version = 4.3.1 (build Sep. 9, 2009 12:30:29)) and imported into Progenesis LC–MS (version 2.4., nonlinear dynamics), which generates a 2D profile of the LC–MS runs. The runs were time aligned with 2–4 user-defined vectors in addition to automated vector aligning using an arbitrarily chosen run as a seed. The runs were stacked and peaks were picked by the software from the stacked data files. Peaks with a charge state of one were removed, at least two isotopes were required, and charge states over +8 were not accepted. The runs were divided into 4 groups; metastatic (3 runs, one from each biological replicate), non-metastatic (3 runs, one from each biological replicate), metastatic non-biotinylated control (1 run) and non-metastatic non-biotinylated control (1 run) followed by comparison of the metastatic and non-metastatic groups against each other. The peptides present in control groups, determined by manual comparison of the peptides, were marked as "not included" in the analysis and further analysis was continued without these peptides. The Progenesis LC–MS normalizes the peptide intensities using proprietary code, and these intensities are used in the statistical analysis. The software calculates ANOVA and q-values, which were used to deduce differentiating peptides. The Progenesis stats-package was used to perform unsupervised principal component analysis (PCA) using the peptides that were not present in the non-biotinylated controls.

For protein identification the peaks were transformed to mgf.-files with Progenesis LC–MS and searched using Mascot (version 2.2, in-house server), Swissprot 2010 (516080 sequences, 181677051 residues) and the following parameters: enzyme: trypsin, peptide mass tolerance: 0.02 Da, fragment mass tolerance 0.8 Da, max missed cleavages 2, variable modifications: carbamidomethy (C), carboxymethyl (C), deamidated (NQ), oxidation (M), propionamide (C), and pyridylethyl (C). The false discovery rate was 3.14% (peptide matches above homology or identity threshold) using decoy database search in Mascot. Individual ion scores >40 indicate identity or extensive homology ($p<0.05$). Same search was also conducted limiting the taxonomy to human, except using variable modifications

carbamidomethyl (C), oxidation (M), and propionamide (C). The false discovery rate was 2.02%. Individual ion scores >25 indicate identity or extensive homology ($p<0.05$). Both results were imported into Progenesis LC–MS as .xml files, and the results were filtered to human proteins. 1104 features were assigned to peptides. Only proteins with Mascot score >40 were accepted as identifications in the total protein list. For the reported differentially expressed proteins at least one unique peptide assigned to them was also required.

2.5. Antibodies

We used the following primary antibodies: anti-PROCR (anti-EPCR, AF2245, R&D Systems Inc. Minneapolis, USA), anti-CD109 (AF4385, R&D Systems Inc., Minneapolis, USA), anti-integrin-α6 (ITGA6, CD49f, BD Pharmingen™, Franklin Lakes, NJ, USA), anti-integrin-β1/CD29 (ITGB1, BAF1778, R&D Systems Inc., Minneapolis, USA), anti-Ecto-ADP-ribosyltransferase 3 (ART3, D01P, Abnova, Taipei City, Taiwan), anti-PTGFRN (s0523, Epitomics, Inc., California, USA and HPA017074, Prestige Antibodies®, Atlas Antibodies, Sweden), anti-Erk1/2 (p44/42 MAPK, 3A7, Cell Signaling Technology Inc., Danvers, MA, USA), anti-β-tubulin (BD Pharmingen™, Franklin Lakes, NJ, USA), anti-BiP (Cell Signaling Technology Inc., Danvers, MA, USA), anti-cytochromec oxidase (Complex IV subunit IV, 20E8C12, Invitrogen, Molecular Probes, Carlsbad, CA, USA) and anti-golgin 97 (CDF4, Invitrogen, Molecular Probes, Carlsbad, CA, USA). Sheep- and rat IgG (Sigma-Aldrich, St. Louis, MO) were used in the control stainings.

2.6. ITGA6 immunoprecipitation and immunoblotting

Cells were covalently biotinylated with the EZ-link® Sulfo-NHS-LC-biotin (Pierce, Rockford, IL, USA) as described in Section 2.2. Lysed cell extracts were centrifuged (20 800×g, at +4 °C). Equal amounts of protein from each extract were pre-cleared using protein G sepharose™ 4 fast flow beads (GE Healthcare Bio-Sciences Ab, Uppsala, Sweden) followed by incubation with 1 μg of the ITGA6 antibodies (+4 °C, o/n) and G sepharose beads (+4 °C, 30 min). Beadswere washed four times with lysis buffer and boiled in *Laemmli* buffer.

For immunoblotting samples (whole cell lysates, cell surface fractions or flow-through fractions representing the unbound proteins, ITGA6 immunoprecipitates) were analyzed using SDS-PAGE and transferred to Immobilon-P Membrane (Millipore, Bedford, MA, USA) for detection. Blots were incubated with the appropriate primary and secondary antibodies (HRP conjugated, Dako, Glostrup, Denmark) or with streptavidin-biotinylated peroxidase complex (Amersham GE Healthcare, Buckinghamshire, UK) and visualized using the SuperSignal West Pico kit (Thermo Fisher Scientific, Pierce, Rockford, IL, USA).

2.7. Xenograft tumors

For the xenograft studies metastatic and non-metastatic cells (1.00E+06) were injected subcutaneously into 4–6 week old female immunocompromised Balb/c nu/nu mice (Taconic, Denmark). Tumors were excised when they reached the size of ≤1 cm^3 and fixed in4% paraformaldehyde (PFA) and prepared for the histological analyses. Animal studies were conducted according to the guidelines of the Provincial Government of Southern Finland, and approved by the Experimental Animal Committee under the permission ESLH-2006-00185/Ym-23.

2.8. Immunofluorescence and immunohistochemistry

To study the expression of the cell surface antigens we used immunofluorescence analyses of live cells. Cells were washed with PBS, non-specific binding was blocked (3% BSA in PBS), and the cells were incubated with the primary antibodies followed by fixation with

4% PFA. Primary antibodies were detected with the appropriate Alexa 594 labeled secondary antibodies (Invitrogen, Molecular Probes, Carlsbad, CA, USA). DNA was visualized with 4′,6-diamino-2-phenylindole (DAPI, Vector Laboratories Inc., Burlingame, CA, USA). The 3D collagen and fibrin cultures were stained and imaged as described [31]. Briefly, cultures were fixed with 4% PFA, blocked with 15% FCS/0.3% Triton-X100/ Dulbecco and stained using the indicated primary antibodies and Alexa Fluor-labeled secondary antibodies. The stainings were mounted with Vectashield anti-fading reagent (Vector Laboratories Inc., Burlingame, CA, USA) and imaged using an AxioImager.Z1 upright epifluorescence microscope with Apotome (Zeiss).

For immunofluorescence analyses of xenograft tumors, frozen tissue sections (8 μM) were stained with the primary antibodies for 1 h at RT followed by the appropriate secondary antibodies. The fluorochromes were visualized with an Axioplan 2 epifluorescence microscope (Zeiss, Jena, Germany) with appropriate filters (Chroma Technology, Rockingham, VT, USA). Image acquisition was performed using a Zeiss digital AxioCamcamera and AxioVision software version AxioVs40 V 4.7.2.0. For the immunohistochemical analyses of paraffin embedded tissues, 4-μm sections were prepared and deparaffinized. The antigens were retrieved using a citrate buffer or trypsin treatment depending on the antibody used. Primary antibodies were detected by using the TSA-kit (Perkin Elmer, Waltham, MA, USA) and the signal was visualized with the AEC-reagent (Sigma-Aldrich, St. Louis, MO). Images were captured with an Olympus DP50 camera and with Olympus Studio Lite software version 1.0 or 1.01.

2.9. Network and pathway analyses

A twofold expression difference (>1.995)was used as a threshold to include proteins in the network and pathway analyses using the computational platform Moksiskaan that integrates six different pathway databases and the Gene Ontology database (http://csbi.ltdk.helsinki.fi/moksiskaan/index.html) [35]. This analysis shows the known downstream targets of alternatively expressed proteins (see Supplemental information S2, metastasis associated proteins for a detailed description). The protein–protein interaction network was pruned to the connections between the genes with an absolute expression correlation greater than 0.4. The expression profiles were taken from The Cancer Genome Atlas breast cancer samples (http://tcga-data.nci.nih.gov/tcga/).

3. Results

3.1. Successful enrichment of cell surface proteins

Several methods have been used for the isolation of plasma membrane proteins. However, the yield of plasma membrane proteins has been low and the majority of the identified proteins have been intracellular [10]. In this work our goal was to optimize a fast and simple enrichment and isolation of cell surface proteins in order to identify novel metastasis associated proteins from a small quantity of starting material. To this end we isolated biotinylated cell surface proteins from an isogenic pair of metastatic and non-metastatic MDA-MB-435 cells using a cleavable, cell impermeable biotin and magnetic streptavidin beads. To diminish the intracellular background seen in the previous studies, we pre-cleared the samples by using biotin agarose beads and included non-biotinylated control samples in the analysis. In addition, we added glycerol to the lysis buffer to prevent the aggregation and increase the solubility of the membrane proteins. Moreover, DNAseI was added to the cell extracts to dissolve the cytosolic actin and proteins associated with it from the viscous DNA in order to liberate a maximal amount of membrane proteins.

These modifications significantly improved the specificity of the cell surface protein isolation. Out of the 86 proteins identified in total from both cell lines (Supplemental Table S1) more than 60% localized to the cell surface/extracellular space according to the Finnish Cell Surface Protein Classifier. To verify the enrichment of cell surface proteins we performed a Western blot analysis of the cell surface fraction as well as of the flow through fraction representing proteins that did not bind to the streptavidin beads i.e. the unbound fraction from the control, non-biotinylated samples as well as from the biotinylated samples. As shown in Fig. 1A a cell surface protein, cluster of differentiation 109 (CD109), was detected only in the biotinylated cell surface fraction while an intracellular protein Erk1/2 was observed only in the unbound fractions. To further confirm the quality of the cell surface protein isolation the biotinylated cell surface fraction and the unbound fraction were analyzed for the presence of the endoplasmic protein BiP, the Golgi protein Golgin 97 and the mitochondrial protein cytochrome C oxidase subunit IV in a Western blot. As shown in Fig. 1B, the cell surface fractions were free of organelle contaminants.

3.2. Differentially expressed proteins were overexpressed in the metastatic cell line and interacted with each other

A Progenesis LC–MS software (Nonlinear Dynamics) was used to identify and quantitate differentially expressed proteins between the two cell lines. This software uses label free quantification of the peptide ion intensities recorded in the MS data collected with data-dependent acquisition. We excluded features present in the control samples and thus representing proteins that bound unspecifically to the magnetic beads from our analysis. The metastatic and non-metastatic cells separated clearly in a principal component analysis (Fig. 1C). Progenesis LC–MS reports the expression differences as the max fold change between the cell lines regardless of which cell line shows a higher expression. A statistically significant expression difference (1.3-fold to 8.8-folds, ANOVA <0.05) was observed for 23/87 proteins (26%; Supplemental Table S1). Table 1 shows the relative expression of differentially expressed proteins as a ratio of metastatic/non-metastatic cells. Based on a Uniprot (http:// www.uniprot.org/) search 18/23 proteins (78%) represented proteins with previously reported cell surface localization. We chose a two-fold difference as a threshold for differential expression and included only these proteins in further analyses. Sixteen proteins showed ≥2-fold expression differences between the cell lines, and interestingly, out of these 14 (87.5%) were overexpressed in the metastatic cells (Table 1).

To study if the identified proteins were involved in similar molecular circuits, we analyzed how they interacted with each other, and which signaling pathways they were involved in using the computational platform Moksiskaan [35]. To simplify the pathways and interactomes we excluded the HLA-molecules from the analyses due to the vast number of different HLAs. We included proteins that showed ≥2-fold expression difference in the Progenesis analysis (Table 1) as up or down regulated. Proteins that showed less than 2-fold expression difference (Table 1) were defined as stable in these analyses. The known relationships between the candidate proteins based on the KEGG pathway analysis are shown in Fig. 2. Gene Ontology analysis using the cellular component ontology showed that our candidate proteins were localized on the cell surface, which further validated the successful enrichment of the cell surface proteins (Supplemental information S2, metastasis associated proteins p. 14). Likewise, metastasis associated *molecular function* terms such as *cell adhesion, integrin mediated signaling pathway*, and *leukocyte migration* were enriched in the metastatic cells (Supplemental information S2, metastasis associated proteins p. 15). Moreover, the KEGG pathway analysis showed differences in several metastasis-associated pathways, such as *gap junctions, focal adhesions*, and *insulin signaling pathway* (Supplemental information S2, metastasis associated proteins p. 5). In addition, one of the two proteins that were significantly downregulated in the metastatic cells was a metastasis

suppressor NME1/Nm23 (Table 1). In the Moksiskaan analysis this gene was associated with *inhibition of cell proliferation*.

3.3. Validation of the differential protein expression in cell lines and in tumor xenografts

To validate the differential expression of metastasis-associated proteins identified in our analysis we selected four novel proteins (prostaglandin F2 receptor negative regulator (PTGFRN/EWI-F/CD9P1), ecto-ADP-ribosyltransferase 3 (ART3), endothelial protein C receptor (PROCR/CD201) and CD109) against those which commercially available antibodies existed. Since these proteins are not well characterized the accessibility of available antibodies was very limited. In the quantitative analysis these proteins differed in their expression seven-, six-, four-, and two-folds, respectively, (Table 1). Out of the selected proteins CD109 and PTGFRN were identified based on 43 and 11 unique peptides while PROCR was identified based on three and ART3 on two unique peptides. The differential expression at the cell surface of the metastatic and non-metastatic MDA-MB-435 cells was confirmed for the PROCR and CD109 in the Western blot analysis. Both showed higher expression in the metastatic cell line (Fig. 3A) in agreement with the Progenesis analysis. Since the differential expression at the cell surface could result either from differences in the expression levels or differential localization of proteins we also analyzed the expression of CD109 and PROCR in whole cell extracts. Both of these proteins were expressed at higher levels in the metastatic cell line compared to the non-metastatic cells (Fig. 3A).

In addition, we selected integrin α6, (ITGA6), which has previously been reported to play a pro-metastatic role in many cancers [36, 37], for validation. Since the anti-ITGA6 antibody did not detect the denatured form of the protein, we performed an immunoprecipitation of the biotinylated cell surface proteins of the metastatic and non-metastatic cells. The biotinylated, immunoprecipitated ITGA6 was then detected using the streptavidin-biotinylated peroxidase complex. The metastatic cells showed higher ITGA6 cell surface levels compared to the non-metastatic ones (Fig. 3A). Integrin β1 (ITGB1) was used as a control since only a 1.4-fold difference in its expression was detected between the metastatic and non-metastatic cells. As anticipated we detected no difference in the expression of ITGB1 in this analysis (Fig. 3A).

To further validate the differential expression we used immunofluorescence staining of the surface of live cells. The metastatic cells expressed more CD109, PROCR, and ITGA6 on their surface than the non-metastatic ones while no difference in the expression of ITGB1 could be detected (Fig. 3B).

The expression of proteins under cell culture conditions does not always correlate with the in vivo conditions [38]. Therefore, we analyzed the expression of CD109, PROCR, ITGA6, and PTGFRN in tumor xenografts derived from the metastatic and non-metastatic MDA-MB-435 cells. The anti-PTGFRN antibodies worked only in this analysis. As shown in Fig. 4 expression of CD109 (A and B), PTGFRN (D and E), PROCR (G and H), and ITGA6 (J and K)was higher in the metastatic tumors compared to the non-metastatic ones validating our cell line results also in an in vivo model. All proteins showed cell surface staining in the tumors suggesting that the localization of the proteins was similar in vitro and in vivo.

The mRNA levels of CD109, PROCR, PTGFRN, and ITGA6 (Goodison et al., unpublished data) corroborated the protein data indicating the transcriptional regulation of the expression of these proteins. Unfortunately, the anti-ART3 antibodies did not work in any of the assays tested (data not shown). However, the mRNA levels of ART3 were significantly higher in the metastatic cells compared to the non-metastatic ones (Goodison et al., unpublished data)

suggesting that the differential expression of ART3 observed in the Progenesis quantitation may also hold true.

3.4. The overexpression of CD109 and ITGA6 marks cells derived from melanoma metastasis

Since PROCR did not show a clear differential expression in tumors and the anti-PTGFRN and anti-ART3 antibodies did not work in immunofluorescence we validated the expression of CD109 and ITGA6 further, and studied their expression in six different melanoma cell lines (WM164, WM165, WM793, WM852, G361 and Bowes). Interestingly, CD109 was highly expressed on the surface of the metastatic melanoma cell lines (WM164, WM165, and WM852) while cells derived from non-metastatic primary melanomas (G361 and Bowes) expressed negligible amounts of CD109 in two-dimensional monolayer cell culture (2D) (Fig. 5, control staining in Supplemental Fig. S2A). Only one cell line of primary melanoma origin, the WM793 cells derived from an invasive advanced vertical growth phase of melanoma, also expressed notable levels of CD109 (Fig. 5). ITGA6 was highly expressed in WM852 cells. In addition, WM793 cells expressed notable amounts of ITGA6, while the rest of the cell lines showed very low or undetectable levels of ITGA6 (data not shown). Importantly, when the cells were implanted inside a three-dimensional (3D) matrix composed of cross-linked fibrin, which typifies the fibrin-rich tumor–stroma interface of melanoma in vivo [39], both ITGA6 and CD109 were highly expressed in the cells derived from melanoma metastasis (Fig. 6, control staining in Supplemental Fig. S2D). WM793 cells from advanced vertical growth phase primary melanoma also expressed detectable levels of CD109 while ITGA6 was essentially undetectable in the cells derived from primary melanomas (Fig. 6). Since the CD109 expression marked the melanoma cells derived from the metastatic site we also studied the expression of CD109 in four invasive and four non-invasive breast cancer cell lines [40]. Interestingly, Western blot analysis revealed that CD109 was preferentially expressed in invasive breast cancer cells. Three out of four invasive cell lines (BT549, HS578T, and SUM159) expressed high levels of CD109. MDA-MB-231 was the only one invasive cell line that showed no detectable CD109 expression. None of the non-invasive breast cancer cell lines (MCF-7, ZR75-1, BT474, and T47D) expressed detectable amounts of CD109 (Supplemental Fig. S1).

4. Discussion

By using shotgun proteomics to compare an isogenic pair of metastatic and non-metastatic cells, we identified novel cell surface proteins associated with cancer metastasis. Our results show that we succeeded in the optimization of enrichment, isolation, and identification of biotinylated cell surface proteins: out of the 86 proteins identified in total more than 60% were localized at the cell surface/extracellular space. Previously, majority of the proteins (59–82%) identified using the biotinylation method have not been classified as true cell surface proteins [10]. Strassberger et al. [41] reported synthesization of a novel, triply charged biotinylation reagent, NHS-b-Ala-(L-Asp) 3-biotin and compared its efficacy in isolation of cell surface proteins to the commercially available sulfo-NHS-LC-biotin in an in vivo analysis of vascular marker proteins. According to their results, this novel reagent labeled the cell surface proteins more specifically than the sulfo-NHS-LC-biotin. It would be interesting to see, if this novel biotinylation reagent would override the commercial biotin also in cell culture. The number of total protein identifications in our study was quite limited. This could partially be explained by the low number of cells (one 100 mm cell culture dish with about 5×10^6 cells) used for the biotinylation and isolation of the cell surface proteins. The low cell number offers, however, some advantages in e.g. analysis of multiple cell lines simultaneously. In addition to the number of cells, performance of repeated LC–MS analyses without exclusion lists to exclude already fragmented features,

exclusion of all peptides present in the control samples, and performance of DB search within the Progenesis LC–MS software with quite a limited number of peptide modifications have all reduced the number of identifications.

In our cell surface analysis we also identified proteins, like the tubulin alpha-1C chain (TUBA1C) and mitochondrial aspartate aminotransferase (GOT2) that are considered intracellular and could be contaminants due to partial purification of our cell surface fractions. However, tubulin was recently reported also to be expressed on the surface of human lymphoid cells of leukemic origin [42, 43] and human monocytic cells [44]. GOT2 is known to be a cell surface fatty acid transporter protein [45, 46]. It is well known that proteins can shuttle between organelles leading to multiple localizations for a single protein [47]. With the aid of more sensitive technologies even a small amount of protein can be detected revealing novel localizations for classical intracellular proteins. Cell surface or plasma membrane localization has already been confirmed for several cytoplasmic, nuclear, and even mitochondrial proteins like grp78 [48], nucleolin [49], annexin [48], heat-shock proteins 90 alpha, hsp70 and gp96 [50, 51], derlin [51], p32 [52], and histone H2B, [53]. For an unknown reason, the extracellular localization of proteins that normally reside inside the cell is not uncommon in tumors. The mechanism of the transport of these intracellular proteins and their function at the cell surface is not known. It might well differ from the protein's function at an intracellular site. These non-classical cell surface proteins might carry post-translational modifications that could affect their function by changing their physical properties, solubility, localization, and interactions with other proteins.

In our label free quantitative analysis we identified 16 proteins displaying over twofold differences in their expression. Only three out of these (HLA-DRB1, HLA-DRA1 and ITGA6) have been identified in the previously reported proteomic analysis of ultracentrifuged and density separated plasma membrane fractions of these same isogenic cancer cell lines [29]. The role of about one-third of the significantly differentially expressed proteins identified in this study is well documented in cancer progression and metastasis. This nicely demonstrates the validity of the cell line model used. High expression of ADAM10 [54] and various integrins [55], which in our analysis were overexpressed in the metastatic cell line, has been shown to promote metastatic growth. NME1, which was down regulated in the metastatic cells, is reported to act as ametastasis suppressor [56]. The rest of the identified proteins have only a few or no reports of association with cancer metastasis in the literature (Table 1). The differential expression of all five proteins (CD109, PROCR, PTGFRN, ITGA6, ART3,) selected for validation could be confirmed in the cell lines either at the protein or at the mRNA level. In addition, the differential expression of HLA-DRB1 and HLA-DRA1 has previously been validated in the proteomic analysis of ultracentrifuged and density separated plasma membrane fractions in these same cells [57]. Taken together, validation of the differential expression of seven out of the sixteen proteins (44%) identified in our analysis demonstrates the reliability of our label free quantitation results. Since the expression levels of proteins in vitro often differ from those in vivo we studied the expression of CD109, PROCR, ITGA6 and PTGFRN in xenograft tumors derived from the metastatic and non-metastatic cells. The differential expression between the two groups of tumors could be confirmed for all of these proteins. PTGFRN was originally reported to associate with and inhibit prostaglandin F2α binding to its receptor [58]. Later on, it has been reported to participate in the tetraspanin web [59–61]. Expression of PTGFRN positively correlates with the metastatic status of human lung tumors [62]. However, the function of PTGFR in the metastatic process warrants further studies.

Interestingly, majority (14/16) of the differentially expressed proteins identified in our analysis were overexpressed in the metastatic cell line compared to the non-metastatic ones. In this respect our results are similar to those from previous proteomic analysis of

ultracentrifuged and density separated plasma membrane fractions of the same isogenic MDA-MB-435 cancer cell lines [29]. In this previous report, eight out of eleven identified significantly differentially expressed cell surface proteins showed higher and three lower expression in the metastatic cell line than in their non-metastatic counterpart. Therefore, the overexpression/localization of certain proteins on the surface of the metastatic cells may help the cells to adapt to the new microenvironment, and facilitate extravasation and colonization at the secondary site. This is supported by the observation that in the Gene Ontology terms adhesion and leukocyte migration were enriched in our pathway analysis of the differentially expressed proteins identified in the current study. Indeed, it has been hypothesized that tumor cells would use similar mechanisms as leukocytes to adhere and extravasate at secondary sites [63]. Moreover, certain chemokine receptors expressed by tumor cells have been shown to promote metastasis, and inhibition of the CXCL12–CXCR4 axis was shown to block metastasis of the MDA-MB-231 cells to the lungs [64].

In our analysis, CD109 was identified as a novel metastasis-associated candidate protein. In 2D and 3D cultures of six melanoma cell lines with distinct invasive potential and origin from primary melanoma or melanoma metastasis [31], CD109 and the known metastasis-associated protein, ITGA6, showed an interesting staining pattern. High CD109 expression was detected in WM852, WM165 and WM793 cell lines in 2D cultures. Most importantly, the 3D cultures of all the cell lines derived from melanoma metastasis (WM852, WM165 and WM164) expressed high levels of both ITGA6 and CD109 while almost no expression of these proteins was detected in the 3D cultures of Bowes and G361 cells derived from primary melanomas. In addition, ITGA6 was essentially undetectable in the WM793 cells derived from the invasive advanced vertical growth phase of primary melanoma, while CD109 expression was detectable also in these cells. Moreover, CD109 was expressed in three out of four invasive breast carcinoma cells. CD109 is a GPI-linked cell surface protein, which negatively modulates TGFB1 signaling in keratinocytes [65, 66]. Expression of its transcript has previously been linked to melanoma in a transgenic melanoma mouse model [67].

As a conclusion, we have optimized the isolation method of the biotinylated cell surface proteins by including to previously reported protocols the addition of glycerol to the lysis buffer, DNAse-treatment of the cell extracts, and pre-clearing of the cell extracts. This clearly reduced the intracellular background detected in the previous studies and allowed us to identify several novel metastasis-associated cell surface proteins. In the future, it will be important to analyze the functional role of these novel proteins in the metastatic process in different types of cancer.

Supplementary Material

Refer to Web version on PubMed Central for supplementary material.

Acknowledgments

We thank Maija Hyvönen and Anastasiya Chernenko for their help with the antibody validation, Rui Li and Flora Naikal for their excellent technical help in preparing the several melanoma and breast carcinoma cell samples for validation, Antti Vaheri and Jorma Keskioja for providing the antibodies, The Cancer Genome atlas for the expression profiles of breast cancer and the staff of the Biomedicum Imaging Unit for their assistance with imaging. This work was supported by grants from the Academy of Finland (Nos. 107664, 124212 and 131732), Finnish Cancer Organizations, University of Helsinki Foundations, and the European Community's Seventh Framework Programme FP7/2007–2011 under grant agreement no 201279. P-RK is supported by the Helsinki Graduate Program in Biotechnology and Molecular Biology, and grants from the K. Albin Johansson and Magnus Ehrnroth Foundations. ML is supported by the Finnish Doctoral Program in Computational Sciences, FICS.

REFERENCES

1. Fidler IJ. The pathogenesis of cancer metastasis: the 'seed and soil' hypothesis revisited. Nat Rev Cancer. 2003; 3(6):453–458. [PubMed: 12778135]
2. Ossowski L, Aguirre-Ghiso JA. Dormancy of metastatic melanoma. Pigment Cell Melanoma Res. 2010; 23(1):41–56. [PubMed: 19843243]
3. Auerbach R, et al. Specificity of adhesion between murine tumor cells and capillary endothelium: an in vitro correlate of preferential metastasis in vivo. Cancer Res. 1987; 47(6):1492–1496. [PubMed: 3815350]
4. Johnson RC, et al. Endothelial cell membrane vesicles in the study of organ preference of metastasis. Cancer Res. 1991; 51(1):394–399. [PubMed: 1988100]
5. Nguyen DX, Bos PD, Massague J. Metastasis: from dissemination to organ-specific colonization. Nat Rev Cancer. 2009; 9(4):274–284. [PubMed: 19308067]
6. Hopkins AL, Groom CR. The druggable genome. Nat Rev Drug Discov. 2002; 1(9):727–730. [PubMed: 12209152]
7. Overington JP, Al-Lazikani B, Hopkins AL. How many drug targets are there? Nat Rev Drug Discov. 2006; 5(12):993–996. [PubMed: 17139284]
8. Brunet S, et al. Organelle proteomics: looking at less to see more. Trends Cell Biol. 2003; 13(12): 629–638. [PubMed: 14624841]
9. Leth-Larsen R, Lund RR, Ditzel HJ. Plasma membrane proteomics and its application in clinical cancer biomarker discovery. Mol Cell Proteomics. 2010; 9(7):1369–1382. [PubMed: 20382631]
10. Elschenbroich S, et al. Isolation of cell surface proteins for mass spectrometry-based proteomics. Expert Rev Proteomics. 2010; 7(1):141–154. [PubMed: 20121483]
11. Rahbar AM, Fenselau C. Integration of Jacobson's pellicle method into proteomic strategies for plasma membrane proteins. J Proteome Res. 2004; 3(6):1267–1277. [PubMed: 15595737]
12. Mathias RA, et al. Tandem application of cationic colloidal silica and Triton X-114 for plasma membrane protein isolation and purification: towards developing an MDCK protein database. Proteomics. 11(7):1238–1253. [PubMed: 21337516]
13. Elia G. Biotinylation reagents for the study of cell surface proteins. Proteomics. 2008; 8(19):4012–4024. [PubMed: 18763706]
14. Wollscheid B, et al. Mass-spectrometric identification and relative quantification of N-linked cell surface glycoproteins. Nat Biotechnol. 2009; 27(4):378–386. [PubMed: 19349973]
15. Ruoslahti E, Rajotte D. An address system in the vasculature of normal tissues and tumors. Annu Rev Immunol. 2000; 18:813–827. [PubMed: 10837076]
16. Brown DM, Ruoslahti E. Metadherin, a cell surface protein in breast tumors that mediates lung metastasis. Cancer Cell. 2004; 5(4):365–374. [PubMed: 15093543]
17. Dowling P, Walsh N, Clynes M. Membrane and membrane-associated proteins involved in the aggressive phenotype displayed by highly invasive cancer cells. Proteomics. 2008; 8(19):4054–4065. [PubMed: 18780347]
18. Brooks SA, et al. Molecular interactions in cancer cell metastasis. Acta Histochem. 2010; 112(1): 3–25. [PubMed: 19162308]
19. Urquidi V, et al. Contrasting expression of thrombospondin-1 and osteopontin correlates with absence or presence of metastatic phenotype in an isogenic model of spontaneous human breast cancer metastasis. Clin Cancer Res. 2002; 8(1):61–74. [PubMed: 11801541]
20. Goodison S, et al. Prolonged dormancy and site-specific growth potential of cancer cells spontaneously disseminated from nonmetastatic breast tumors as revealed by labeling with green fluorescent protein. Clin Cancer Res. 2003; 9(10 Pt 1):3808–3814. [PubMed: 14506175]
21. Ellison G, et al. Further evidence to support the melanocytic origin of MDA-MB-435. Mol Pathol. 2002; 55(5):294–299. [PubMed: 12354931]
22. Rae JM, et al. MDA-MB-435 cells are derived from M14 melanoma cells—a loss for breast cancer, but a boon for melanoma research. Breast Cancer Res Treat. 2007; 104(1):13–19. [PubMed: 17004106]

23. Ross DT, et al. Systematic variation in gene expression patterns in human cancer cell lines. Nat Genet. 2000; 24(3):227–235. [PubMed: 10700174]
24. Chambers AF. MDA-MB-435 and M14 cell lines: identical but not M14 melanoma? Cancer Res. 2009; 69(13):5292–5293. [PubMed: 19549886]
25. Hollestelle A, Schutte M. Comment re: MDA-MB-435 and M14 cell lines: identical but not M14 melanoma? Cancer Res. 2009; 69(19):7893. [PubMed: 19723654]
26. Schwirzke M, et al. Identification of metastasis-associated genes by transcriptional profiling of a pair of metastatic versus non-metastatic human mammary carcinoma cell lines. Anticancer Res. 2001; 21(3B):1771–1776. [PubMed: 11497258]
27. Kreunin P, et al. Identification of metastasis-associated proteins in a human tumor metastasis model using the mass-mapping technique. Proteomics. 2004; 4(9):2754–2765. [PubMed: 15352249]
28. Kreunin P, et al. Proteomic profiling identifies breast tumor metastasis-associated factors in an isogenic model. Proteomics. 2007; 7(2):299–312. [PubMed: 17205601]
29. Lund R, et al. Efficient isolation and quantitative proteomic analysis of cancer cell plasma membrane proteins for identification of metastasis-associated cell surface markers. J Proteome Res. 2009; 8(6):3078–3090. [PubMed: 19341246]
30. Pasquali C, Fialka I, Huber LA. Subcellular fractionation, electromigration analysis and mapping of organelles. J Chromatogr B Biomed Sci Appl. 1999; 722(1–2):89–102. [PubMed: 10068135]
31. Tatti O, et al. Membrane-type-3 matrix metalloproteinase (MT3-MMP) functions as a matrix composition-dependent effector of melanoma cell invasion. PLoS One. 2011; 6(12):e28325. [PubMed: 22164270]
32. Scheurer SB, et al. Identification and relative quantification of membrane proteins by surface biotinylation and two-dimensional peptide mapping. Proteomics. 2005; 5(11):2718–2728. [PubMed: 15986331]
33. Roesli C, et al. Identification of the surface-accessible, lineage-specific vascular proteome by two-dimensional peptide mapping. FASEB J. 2008; 22(6):1933–1944. [PubMed: 18180333]
34. Kinter, M.; Sherman, NE. Protein sequencing and identification using tandem mass spectrometry. New York: John Wiley & Sons, Inc; 2000. p. 160-163.
35. Laakso M, Hautaniemi S. Integrative platform to translate gene sets to networks. Bioinformatics. 2010; 26(14):1802–1803. [PubMed: 20507894]
36. Wang Y, et al. Integrin subunits alpha5 and alpha6 regulate cell cycle by modulating the chk1 and Rb/E2F pathways to affect breast cancer metastasis. Mol Cancer. 2011; 10:84. [PubMed: 21752283]
37. Demetriou MC, Cress AE. Integrin clipping: a novel adhesion switch? J Cell Biochem. 2004; 91(1):26–35. [PubMed: 14689578]
38. Wick N, et al. Transcriptomal comparison of human dermal lymphatic endothelial cells ex vivo and in vitro. Physiol Genomics. 2007; 28(2):179–192. [PubMed: 17234577]
39. Wojtukiewicz MZ, et al. Malignant melanoma. Interaction with coagulation and fibrinolysis pathways in situ. Am J Clin Pathol. 1990; 93(4):516–521. [PubMed: 1690950]
40. Neve RM, et al. A collection of breast cancer cell lines for the study of functionally distinct cancer subtypes. Cancer Cell. 2006; 10(6):515–527. [PubMed: 17157791]
41. Strassberger V, et al. A novel reactive ester derivative of biotin with reduced membrane permeability for in vivo biotinylation experiments. Proteomics. 2010; 10(19):3544–3548. [PubMed: 20821733]
42. Rubin RW, et al. Tubulin as a major cell surface protein in human lymphoid cells of leukemic origin. Cancer Res. 1982; 42(4):1384–1389. [PubMed: 6949640]
43. Quillen M, et al. Cell surface tubulin in leukemic cells: molecular structure, surface binding, turnover, cell cycle expression, and origin. J Cell Biol. 1985; 101(6):2345–2354. [PubMed: 4066762]
44. Por SB, et al. Antibodies to tubulin and actin bind to the surface of a human monocytic cell line, U937. J Histochem Cytochem. 1991; 39(7):981–985. [PubMed: 1865114]

45. Stump DD, Zhou SL, Berk PD. Comparison of plasma membrane FABP and mitochondrial isoform of aspartate aminotransferase from rat liver. Am J Physiol. 1993; 265(5 Pt 1):G894–G902. [PubMed: 8238519]
46. Bradbury MW, Berk PD. Mitochondrial aspartate aminotransferase: direction of a single protein with two distinct functions to two subcellular sites does not require alternative splicing of the mRNA. Biochem J. 2000; 345(Pt 3):423–427. [PubMed: 10642497]
47. Yates III JR, et al. Proteomics of organelles and large cellular structures. Nat Rev Mol Cell Biol. 2005; 6(9):702–714. [PubMed: 16231421]
48. Arap MA, et al. Cell surface expression of the stress response chaperone GRP78 enables tumor targeting by circulating ligands. Cancer Cell. 2004; 6(3):275–284. [PubMed: 15380518]
49. Christian S, et al. Nucleolin expressed at the cell surface is a marker of endothelial cells in angiogenic blood vessels. J Cell Biol. 2003; 163(4):871–878. [PubMed: 14638862]
50. Eustace BK, Jay DG. Extracellular roles for the molecular chaperone, hsp90. Cell Cycle. 2004; 3(9):1098–1100. [PubMed: 15326368]
51. Melendez K, et al. Heat shock protein 70 and glycoprotein 96 are differentially expressed on the surface of malignant and nonmalignant breast cells. Cell Stress Chaperones. 2006; 11(4):334–342. [PubMed: 17278882]
52. Fogal V, et al. Mitochondrial/cell-surface protein p32/gC1qR as a molecular target in tumor cells and tumor stroma. Cancer Res. 2008; 68(17):7210–7218. [PubMed: 18757437]
53. Qiu H, Wang Y. Quantitative analysis of surface plasma membrane proteins of primary and metastatic melanoma cells. J Proteome Res. 2008; 7(5):1904–1915. [PubMed: 18410138]
54. Klein T, Bischoff R. Active metalloproteases of the A Disintegrin and Metalloprotease (ADAM) family: biological function and structure. J Proteome Res. 10(1):17–33. [PubMed: 20849079]
55. Desgrosellier JS, Cheresh DA. Integrins in cancer: biological implications and therapeutic opportunities. Nat Rev Cancer. 2010; 10:9–22. [PubMed: 20029421]
56. Hartsough MT, Steeg PS. Nm23/nucleoside diphosphate kinase in human cancers. J Bioenerg Biomembr. 2000; 32(3):301–308. [PubMed: 11768314]
57. Leth-Larsen R, et al. Metastasis-related plasma membrane proteins of human breast cancer cells identified by comparative quantitative mass spectrometry. Mol Cell Proteomics. 2009; 8(6):1436–1449. [PubMed: 19321434]
58. Orlicky DJ. Negative regulatory activity of a prostaglandin F2 alpha receptor associated protein (FPRP). Prostaglandins Leukot Essent Fatty Acids. 1996; 54(4):247–259. [PubMed: 8804121]
59. Charrin S, et al. The major CD9 and CD81 molecular partner. Identification and characterization of the complexes. J Biol Chem. 2001; 276(17):14329–14337. [PubMed: 11278880]
60. Charrin S, et al. Multiple levels of interactions within the tetraspanin web. Biochem Biophys Res Commun. 2003; 304(1):107–112. [PubMed: 12705892]
61. Stipp CS, Orlicky D, Hemler ME. FPRP, a major, highly stoichiometric, highly specific CD81- and CD9-associated protein. J Biol Chem. 2001; 276(7):4853–4862. [PubMed: 11087758]
62. Guilmain W, et al. CD9P-1 expression correlates with the metastatic status of lung cancer, and a truncated form of CD9P-1, GS-168AT2, inhibits in vivo tumour growth. Br J Cancer. 2011; 104(3):496–504. [PubMed: 21206492]
63. Miles FL, et al. Stepping out of the flow: capillary extravasation in cancer metastasis. Clin Exp Metastasis. 2008; 25(4):305–324. [PubMed: 17906932]
64. Muller A, et al. Involvement of chemokine receptors in breast cancer metastasis. Nature. 2001; 410(6824):50–56. [PubMed: 11242036]
65. Finnson KW, et al. Identification of CD109 as part of the TGF-beta receptor system in human keratinocytes. FASEB J. 2006; 20(9):1525–1527. [PubMed: 16754747]
66. Hagiwara S, et al. Processing ofCD109 by furin and its role in the regulation of TGF-beta signaling. Oncogene. 29(15):2181–2191. [PubMed: 20101215]
67. Ohshima Y, et al. CD109 expression levels in malignant melanoma. J Dermatol Sci. 57(2):140–142. [PubMed: 20034764]

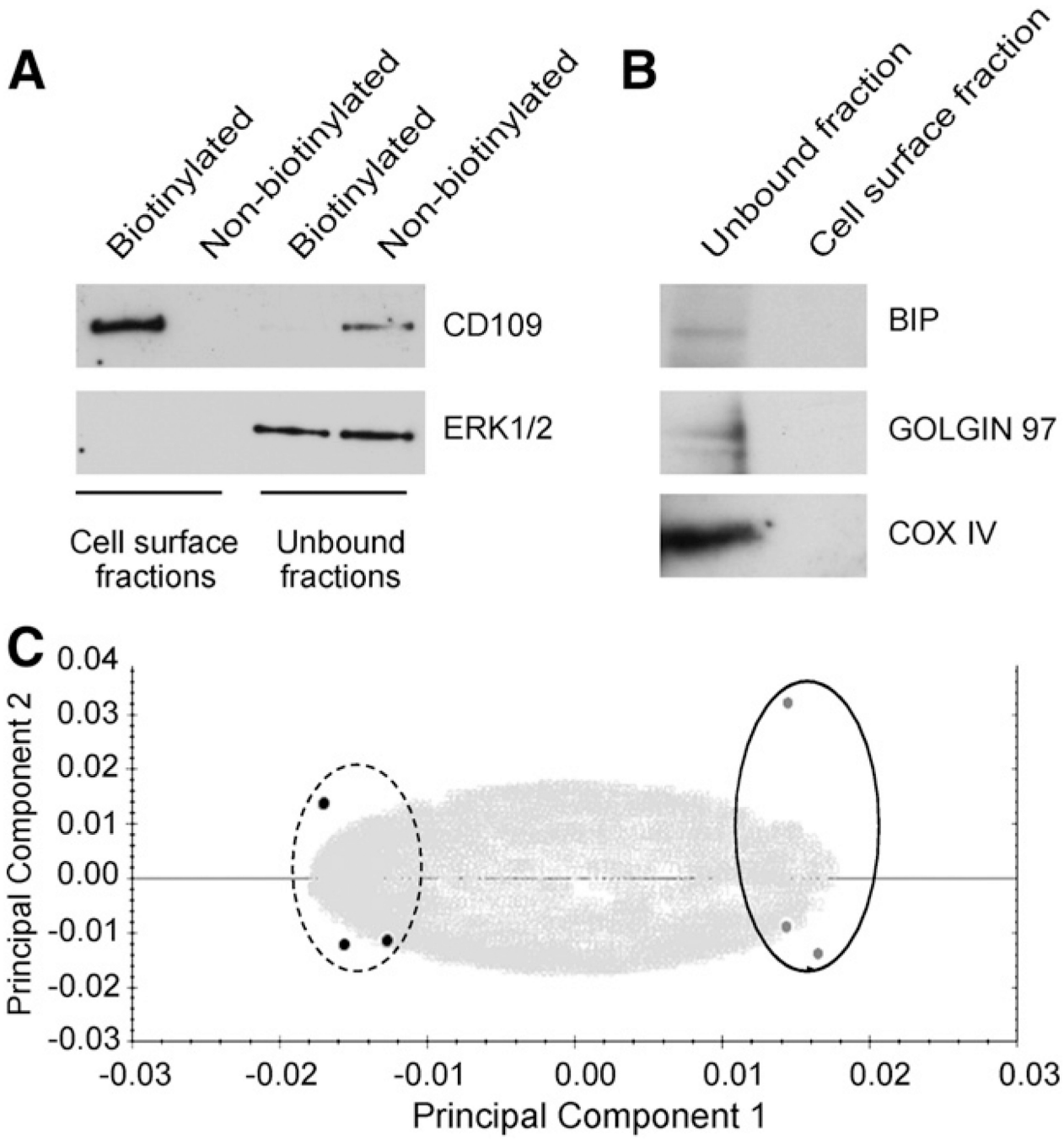

Fig. 1.

Successful isolation of cell surface proteins without contaminants from the organelles. A. Western blot analysis of the cell surface fractions and the flow through (unbound fraction representing proteins that did not bind to the streptavidin beads) was performed from the biotinylated as well as from the non-biotinylated extracts for the presence of a cell surface protein CD109 and an intracellular protein Erk1/2. B. Western blot analysis of the cell surface and the unbound fractions of biotinylated cell extracts shows that the intracellular organelle proteins BiP, Golgin 97, and cytochrome C oxidase subunit IV (COX IV) were only detected in the unbound but not in the cell surface fraction. C. Metastatic (dotted line)

and non-metastatic (solid line) cell surface extracts clearly separated from each other in the Progenesis LC–MS principal component analysis.

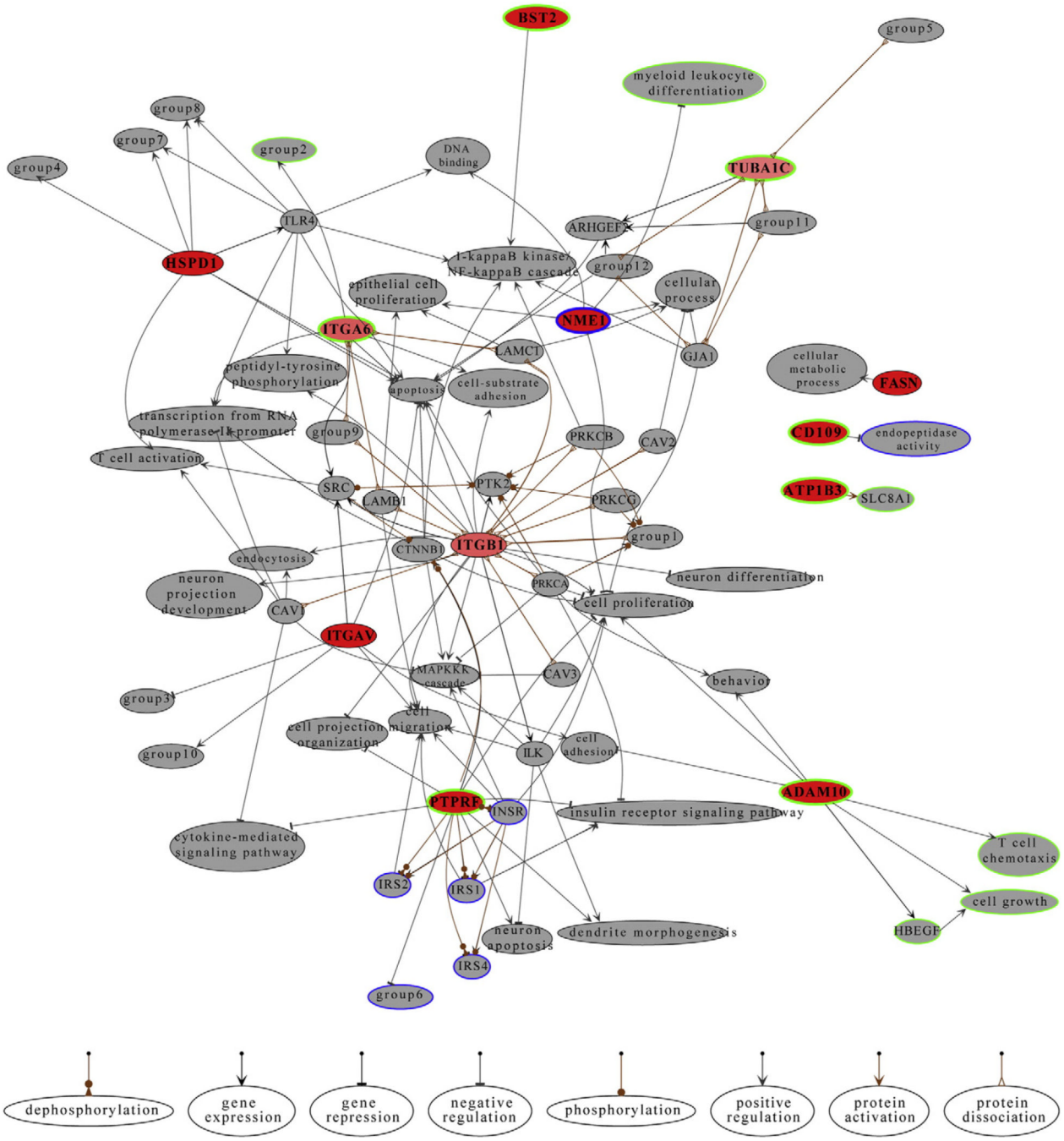

Fig. 2.

Known relationships between the candidate genes. Candidate genes are shown in red if they have only output connections. The ratio of input and output connections determines how thin they are. Completely white genes have only input connections. The network of candidate genes was expanded by fetching genes 1 step downstream. The downstream genes are shown in gray. Nodes that share all their connections and properties were combined in order to reduce the complexity of the graph. The joint nodes are labeled with group# and the participating entities are as follows: group1 = ACTB, ACTG1; group2 = cell–cell adhesion, phosphorylation; group3 = cellular protein metabolic process, lipid storage, lipid transport, lipoprotein metabolic process, low-density lipoprotein particle receptor biosynthetic process,

macrophage derived foam cell differentiation; group4 = cysteine-type endopeptidase activity, interleukin-12 production, macrophage activation, T cell mediated immune response to tumor cell; group5 = DYNC1H1, DYNC1I1, DYNC1I2, DYNC1LI1, DYNC1LI2, DYNC2H1; group6 = epidermal growth factor receptor signaling pathway, nerve growth factor receptor signaling pathway; group7 = innate immune response, interferon-alpha production, interleukin-10 production; group8 = interferon-gamma production, interleukin-6 production; group9 = LAMA1, LAMA2, LAMA3, LAMA4, LAMA5, LAMB2, LAMB3, LAMB4, LAMC2, LAMC3; group10 = osteoblast proliferation, phagocytosis; group11 = RP11-631M21.2, TUBB1, TUBB2A, TUBB2B, TUBB3, TUBB4, TUBB4Q, TUBB6; group12 = TUBB, TUBB2C. Green and blue borders refer to up and down regulated genes, respectively. Light gray is used to emphasize stably expressed genes. Known regulations are shown with bold borders whereas the predictions are kept thin. (For interpretation of the references to color in this figure legend, the reader is referred to the web version of this article.)

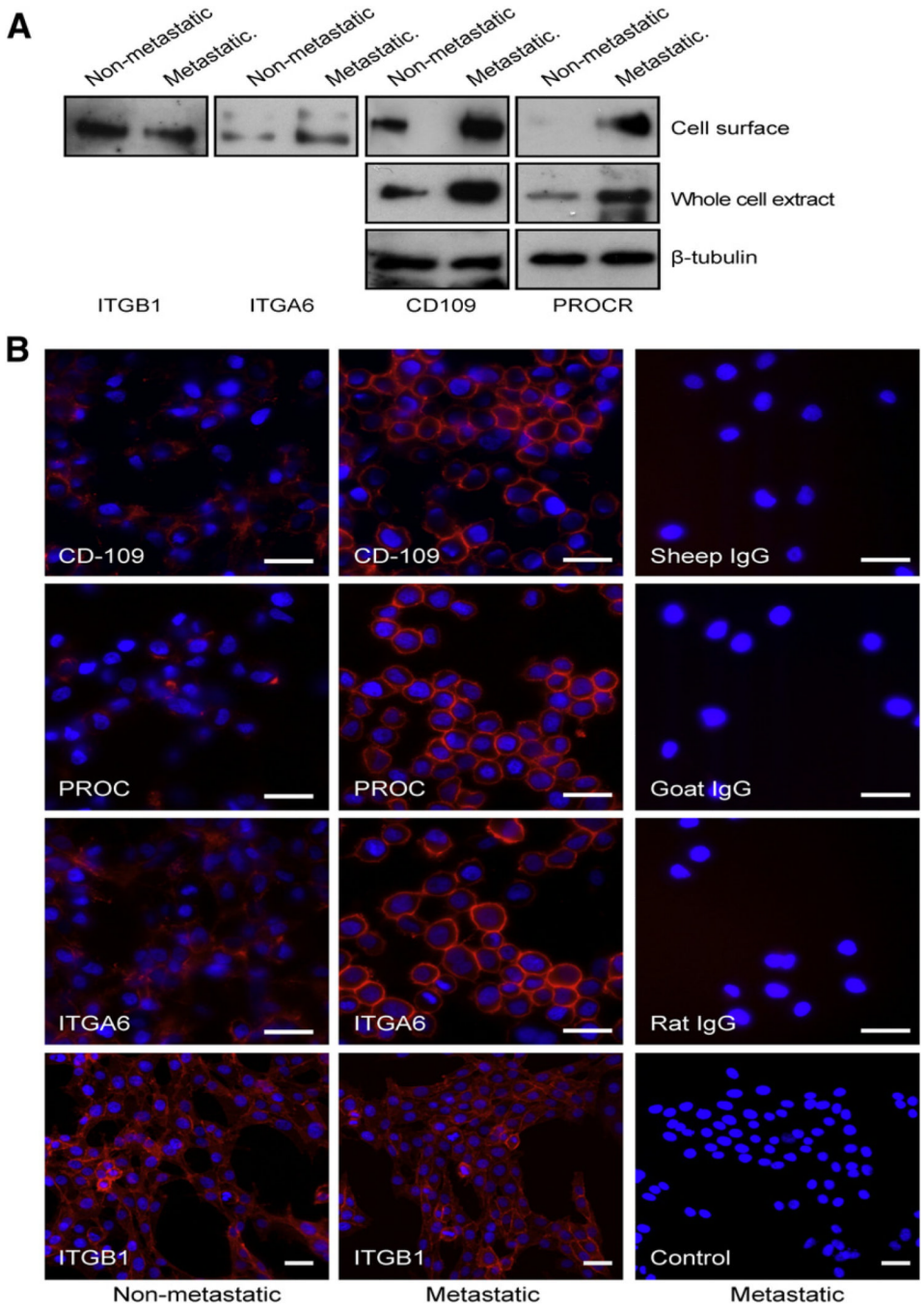

Fig. 3.

Validation of the quantitative differences in the non-metastatic and metastatic cells. A. Expression of CD109, PROCR, ITGA6, and ITGB1 in the metastatic and non-metastatic cells was detected using the Western blot analysis of cell surface extracts. Expression of CD109 and PROCR was also analyzed in the whole cell extracts. Beta-tubulin was used as a loading control for the whole cell extracts. B. Visualization of the cell surface of non-fixed, live non-metastatic and metastatic cells with immunofluorescence using antibodies against CD109, PROCR, ITGA6 and ITGB1 followed by an Alexa-594 conjugated secondary antibody. Metastatic cells showed higher expression of CD109, PROCR, and ITGA6 (red) on their surface than the non-metastatic cells while no difference was observed for ITGB1

between the cell lines. The appropriate control IgGs were used to show the background of the assay (panels in the right). Nuclei were visualized with DAPI (blue). Original magnification 400× (CD109, PROCR, and ITGA6, and their controls) and 200× (ITGB1 and its control). Scale bar 20 μm. Images were digitally cropped in Photoshop CS4. (For interpretation of the references to color in this figure legend, the reader is referred to the web version of this article.)

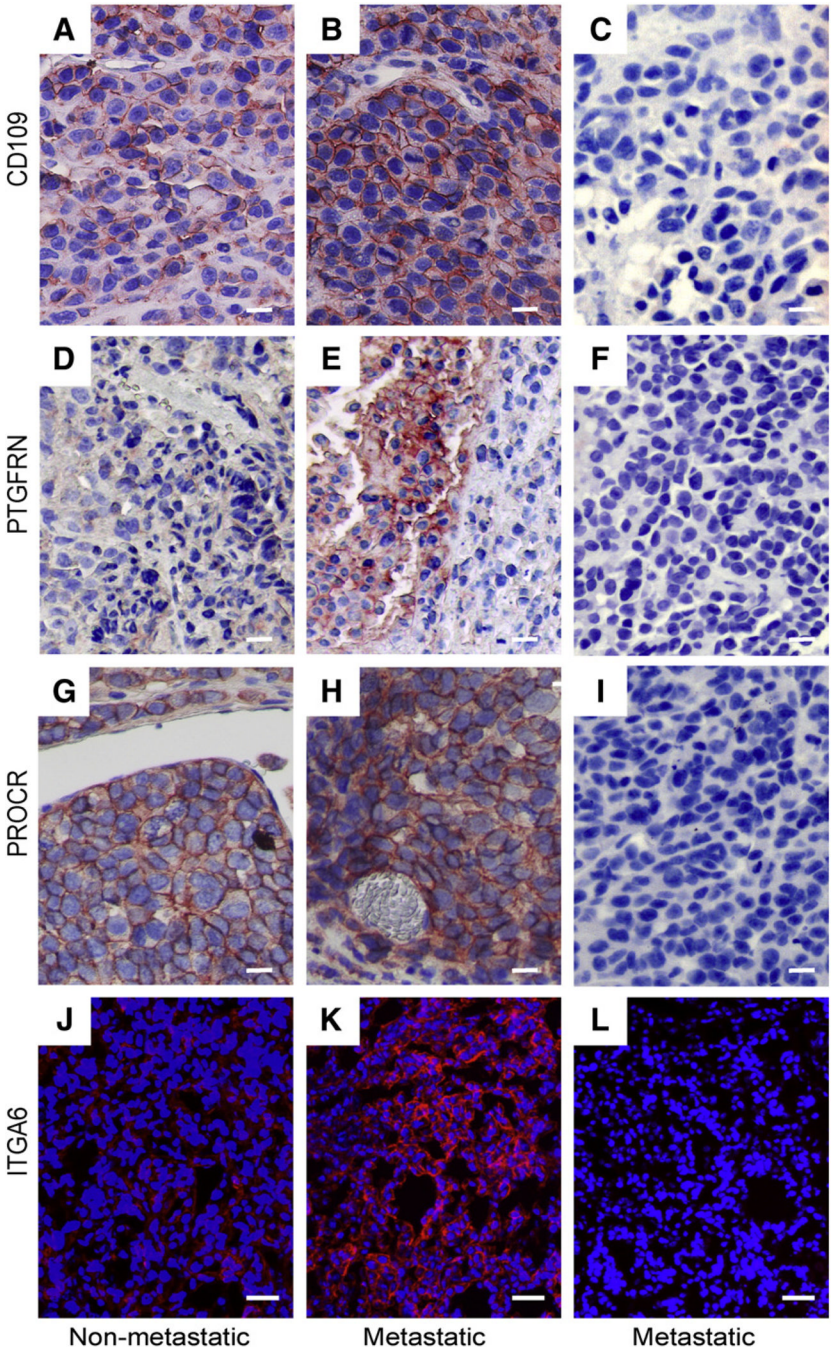

Fig. 4.

Expression of CD109, PTGFRN, PROCR, and ITGA6 in xenograft tumors. Non-metastatic and metastatic cells were implanted subcutaneously in the abdominal area of immunosuppressed mice. Tumors were excised and prepared for histological analyses. Higher expression of CD109 (B), PTGFRN (E), PROCR (H), and ITGA6 (K) was detected in the metastatic tumors than in the non-metastatic ones (A, D, G, and J). The appropriate control IgGs were used to show the background of the assay (C, F, I, and L). In paraffin embedded sections (A–F) primary antibodies were detected by using the TSA-kit and the signal was visualized with the AEC-reagent. Cryo sections (G–H) were stained for the presence of ITGA6 (red) using anti-ITGA6 antibodies followed by an Alexa-594 conjugated

secondary antibody. Nuclei were visualized with DAPI (blue). Original magnification of A–I, 200×; J–L, 100×. Scale bar 20 μm. Images were digitally cropped in Photoshop CS4. (For interpretation of the references to color in this figure legend, the reader is referred to the web version of this article.)

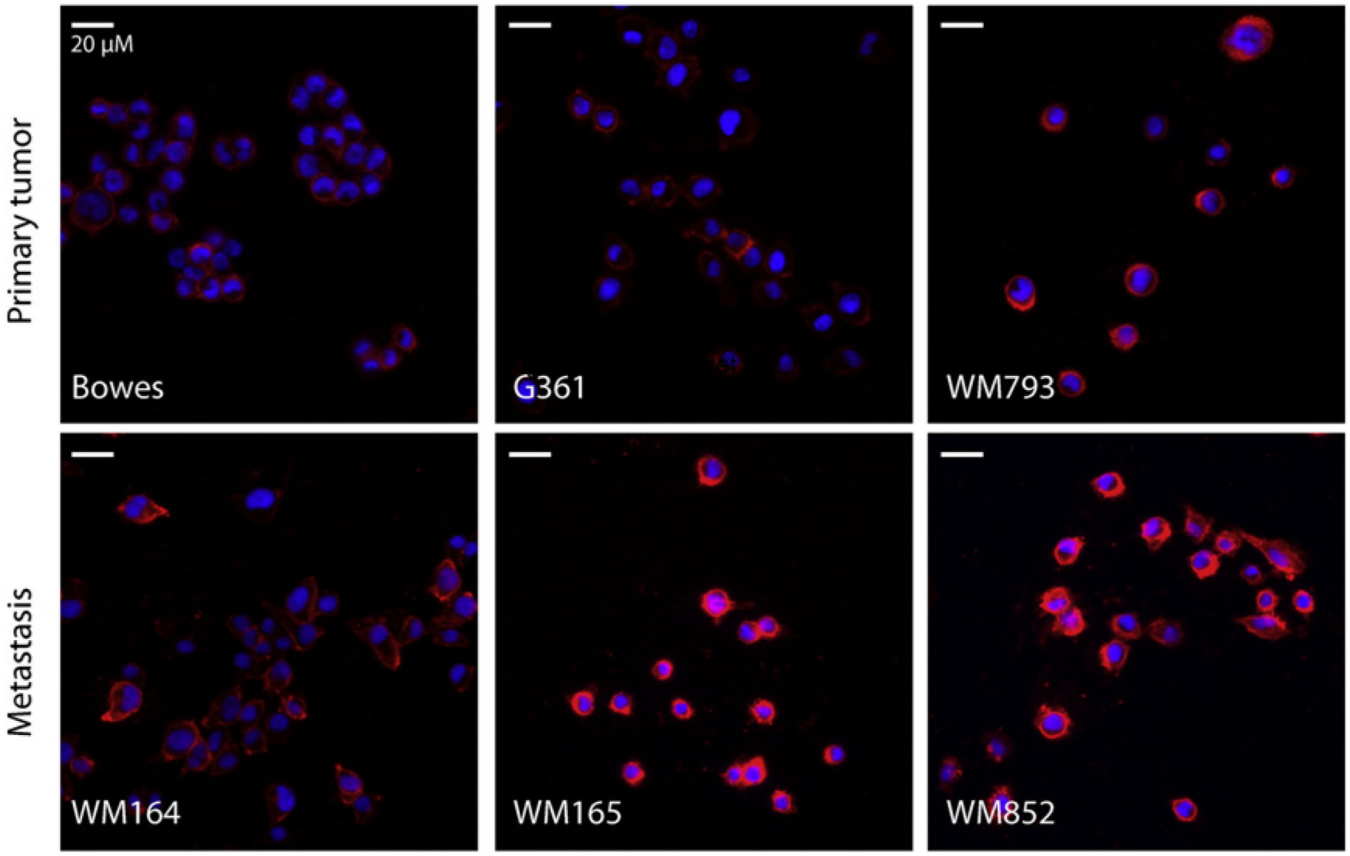

Fig. 5.

Expression of CD109 in different melanoma cell lines. Cells were cultured on the glass cover slips for 2 days prior to staining of the cell surface of non-fixed live cells with an antibody against CD109. CD109 (red) was expressed on the surface of cells derived from melanoma metastasis (WM165, WM164 and WM852) but not on the surface of cells derived from primary melanoma (Bowes and G361). In addition, cells derived from an invasive advanced vertical growth phase of primary melanoma (WM793) expressed detectable levels of CD109. Nuclei were visualized with DAPI (blue). Original magnification 200×. Images were digitally cropped in Photoshop CS4. (For interpretation of the references to color in this figure legend, the reader is referred to the web version of this article.)

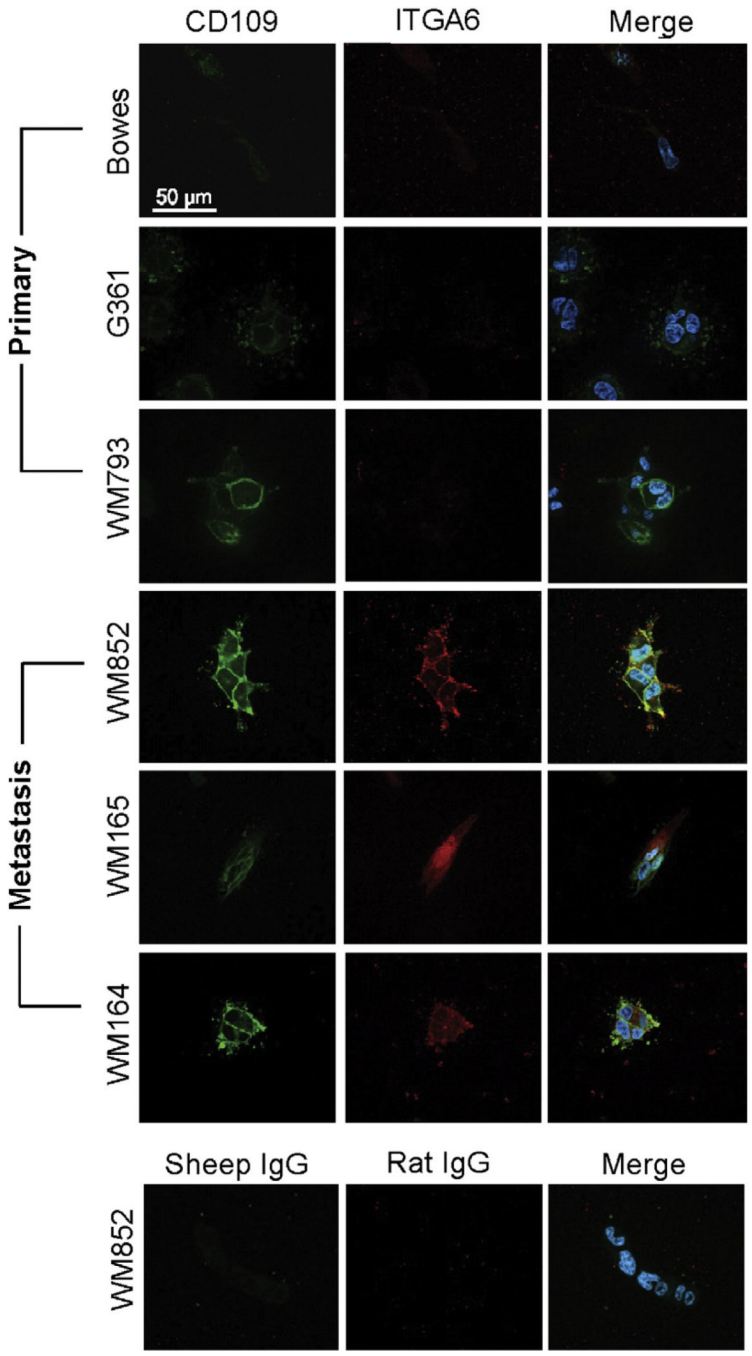

Fig. 6.

CD109 and ITGA6 mark the cells derived from melanoma metastasis in a three-dimensional (3D) fibrin matrix. The melanoma cell lines were embedded in 3D fibrin gels. After 4 days the cultures were fixed and stained with antibodies against CD109 (green) and ITGA6 (red). Nuclei were visualized using DAPI staining (blue). CD109 was expressed in cells from melanoma metastasis (WM165, WM164 and WM852) and in cells from an invasive advanced vertical growth phase of primary melanoma (WM793) but not in cells derived from primary melanoma (Bowes and G361). ITGA6 showed a similar staining pattern than CD109 except that the WM793 cells did not express detectable amounts of ITGA6. The appropriate control IgGs were used to show the background of the assay. Scale bar 50 µm.

(For interpretation of the references to color in this figure legend, the reader is referred to the web version of this article.)

J Proteomics. Author manuscript; available in PMC 2013 December 21.

Table 1

Differentially expressed proteins.

Name	Max. fold change [a]	Score	Peptide count (unique)	ANOVA	Surface/ extracellular	Associated with invasion/metastasis in literature (PubMed search)
HLA-DRB1	**8.8**	337.14	7 (3)	<0.001	Yes	Yes
HLA-DRA1	**2.53**	384.7	7 (2)	0.002	Yes	Yes
BST2	**7.88**	78.83	2 (2)	0.008	Yes	No or little previous connections
PTGFRN	**7.44**	450.26	12 (11)	0.002	Yes	No or little previous connections
ART3	**6.03**	104.26	2 (2)	<0.001	Yes	No or little previous connections
PROCR	**4.40**	95.32	3 (3)	0.002	Yes	No or little previous connections
GPR56	**3.01**	309.42	4 (4)	0.014	Yes	No or little previous connections
ADAM10	**2.74**	170.07	4 (3)	0.006	Yes	Yes
PTPRF	**2.40**	84.68	4 (2)	0.005	Yes	No or little previous connections
ATP1B3	**2.21**	83.49	3 (3)	0.006	Yes	No or little previous connections
CD109	**2.11**	3412.93	51 (43)	0.012	Yes	No or little previous connections
ITGA6	**2.08**	259.05	8 (6)	0.014	Yes	Yes
TUBA1C	**2.01**	71.44	3 (2)	0.005	No	No or little previous connections
IGSF8	**2.00**	357.87	6 (5)	0.022	Yes	No or little previous connections
ITGAV	1.82	544.26	10 (8)	0.007	Yes	Yes
HSPD1	1.76	519.51	6 (5)	0.017	No	No or little previous connections
FASN	1.70	132.38	9 (4)	0.002	No	Yes
ITGB1	1.44	1272.28	21 (13)	0.033	Yes	Yes
GOT2	0.43	196.61	4 (3)	0.004	Yes	No or little previous connections
NME1	0.49	116.90	2 (1)	0.022	No	Yes
CHL1	0.56	55.28	2 (1)	0.007	Yes	No or little previous connections
CD97	0.73	483.97	5 (4)	0.023	Yes	No or little previous connections
ALDH7A1	0.75	209.90	5 (3)	0.043	No	No or little previous connections

[a]Fold difference is shown as a ratio of metastatic/non-metastatic cells.